Nicotinic Acetylcholine Receptor Subunits in Rhesus Monkey Retina

Ji Liu,[1] Alice M. McGlinn,[1] Alcides Fernandes,[2] Ann H. Milam,[1] Christianne E. Strang,[3] Margot E. Andison,[3] Jon M. Lindstrom,[4] Kent T. Keyser,[3] and Richard A. Stone[1]

Purpose. The purpose of this study was to detect and establish the cellular localizations of nicotinic acetylcholine receptor (nAChR) subunits in Rhesus monkey retina.

Methods. Retinas were dissected from the eyes of monkeys killed after unrelated experiments. RNA was extracted and analyzed by RT-PCR, using primers designed against human sequences of α3-α7, α9, and β2-β4 nAChR subunits. The RT-PCR products were separated by gel electrophoresis and sequenced. Frozen sections of postmortem fixed monkey eyes were immunolabeled with well-characterized and specific monoclonal antibodies against the α3, α4, α6, α7, β2, or β4 nAChR subunits and visualized with fluorescence labeling.

Results. Products of the predicted size for the α3-α7, α9, and β2-β4 nAChR subunits were detected by RT-PCR in Rhesus monkey retina. Homology between transcripts from monkey retina and human nucleotide sequences ranged from 93 to 99%. Immunohistochemical studies demonstrated that neurons in various cell layers of monkey retina expressed α3, α4, α7, or β2 nAChR subunits and cells with the morphology of microglia were immunoreactive for the α6 or β4 nAChR subunits.

Conclusions. nAChR subunits are expressed in the monkey retina and localize to diverse retinal neurons as well as putative microglia. Besides mediating visual processing, retinal nAChRs may influence refractive development and ocular pathologies such as neovascularization. (*Invest Ophthalmol Vis Sci.* 2009; 50:1408–1415) DOI:10.1167/iovs.08-2398

Acetylcholine (ACh) activates both nicotinic and muscarinic acetylcholine receptors (AChRs). The nicotinic AChRs (nAChRs) are ligand-gated cation channels and consist of pentameric complexes either composed of subunits α2-α6 and β2-β4 as α/β combinations or composed of subunits α7-α10 as homomeric or heteromeric structures.[1–3] Two broad classes of nAChRs are recognized in brain. One class consists of heteromeric nAChR subtypes comprised of the α2-α6 and β2-β4 units with high agonist affinity but insensitivity to the snake toxin α-bungarotoxin (αBgt); the second class consists of homomeric (i.e., α7, α8, or α9) or heteromeric pentamers (i.e., combined α7, α8, α9, or α10 subunits) with lower agonist affinity but with high sensitivity to αBgt.[3,4] The subunit compositions of nAChRs, which govern their pharmacological and functional properties, vary in different regions of the nervous system.

In the mammalian retina, the cholinergic cells comprise two populations of amacrine cells, with somata in the inner nuclear layer (INL) or ganglion cell layer (GCL) respectively.[5,6] The dendrites of the cholinergic INL cells stratify as a narrow band in the outer portion of the inner plexiform layer (IPL), and those of the cholinergic cells in the GCL stratify as a narrow band in the inner portion of the IPL. Functionally OFF cells, the cholinergic cells in the INL release ACh at the cessation or decrement of light stimulation[5,6]; functionally ON cells, the cholinergic cells in the GCL release ACh at light onset or increment.[7]

Ach, acetylcholinesterase inhibitors, or other cholinergic agents affect the response properties of many types of ganglion cells, including ON- and OFF-center ganglion cells and all motion sensitive ganglion cells.[5,8–12] Based on electrophysiology, many of the retinal actions of ACh are mediated by nAChRs.[8,13] That the application of ACh also decreases responses in the optic nerve likely reflects its summed effect on the activity of various ganglion cells.[13]

In rabbit retina, for instance, both αBgt-sensitive and αBgt-insensitive nAChRs modulate the light responses of subsets of ganglion cell types, including directionally selective ganglion cells as well as many subsets of brisk transient and brisk sustained ganglion cells.[14–18] Both AChR classes are expressed by some ganglion cells, and there is evidence that nAChRs are expressed by upstream cells as well. For example, many ganglion cells and several types of amacrine cells express αBgt-insensitive β2-containing nAChRs, some of which are in combination with α3 and possibly other subunits.[19–21] Furthermore, αBgt-sensitive α7 nAChRs are expressed by rabbit cone bipolar, amacrine, and ganglion cells,[22] suggesting that activation of α7 nAChRs by ACh may affect information processing in multiple retinal circuits. Consistent with inner retinal localization of nAChRs, physiological studies demonstrate that the frog ERG b-wave is inhibited by ACh,[23] possibly through a cholinergic-glycinergic feedback loop[24,25]; the cat b-wave is first enhanced and then rapidly inhibited by ACh,[26] suggesting the activation of multiple upstream nAChR subtypes. In rhesus monkey, the pattern ERG is enhanced by the ACh precursor L-α-glyceryl-phosphorylcholine.[27]

Although cholinergic mechanisms mediated by nAChRs also influence experimental retinal neovascularization[28] and are involved in refractive development,[29–31] a major gap in understanding the role of ACh in the normal and diseased retina is the limited information concerning the expression of nAChRs in non-human primate and human retinas. We report the results of RT-PCR and immunohistochemical studies of nAChR subunit expression in Rhesus monkey retina and discuss these

From the [1]Department of Ophthalmology, Scheie Eye Institute, and the [4]Department of Neurosciences, University of Pennsylvania, Philadelphia, Pennsylvania; [2]Yerkes National Primate Research Center, Department of Ophthalmology, Emory University, Atlanta, Georgia; and [3]Vision Science Research Center, University of Alabama at Birmingham, Birmingham, Alabama.

Supported by Philip Morris USA Postdoctoral Fellowship of the Philip Morris External Research Program (JL); NIH Grants R01-EY-07354 (RAS), R01-EY-07845 (KTK), P30-EY-03039 (KTK); the Paul and Evanina Bell Mackall Foundation Trust (AHM, RAS); and Research to Prevent Blindness (RAS).

Submitted for publication June 6, 2008; revised September 24, 2008; accepted January 20, 2009.

Disclosure: **J. Liu**, None; **A.M. McGlinn**, None; **A. Fernandes**, None; **A.H. Milam**, None; **C.E. Strang**, None; **M.E. Andison**, None; **J.M. Lindstrom**, None; **K.T. Keyser**, None; **R.A. Stone**, None

The publication costs of this article were defrayed in part by page charge payment. This article must therefore be marked "*advertisement*" in accordance with 18 U.S.C. §1734 solely to indicate this fact.

Corresponding author: Richard A. Stone, D-603 Richards Bldg., University of Pennsylvania School of Medicine, Philadelphia, PA 19104-6075; stone@mail.med.upenn.edu.

Investigative Ophthalmology & Visual Science, March 2009, Vol. 50, No. 3

findings in comparison to previous observations in the retinas of other mammals.

Materials and Methods

Monkey eyes were enucleated after death from Rhesus monkeys killed at the conclusion of unrelated experiments at the Yerkes National Primate Research Center. Animal treatment conformed to the ARVO Statement for the Use of Animals in Ophthalmic and Vision Research.

RNA Isolation and Amplification

Intact retinas were dissected into RNA stabilizing solution (RNAlater; Ambion, Austin, TX) immediately after enucleation. RNA was extracted using a purification kit (Absolutely RNA RT-PCR Miniprep Kit; Stratagene, La Jolla, CA). Briefly, tissue was homogenized in lysis buffer containing guanidine thiocyanate and β-mercaptoethanol. The homogenates were pre-filtered, and captured onto a fiber matrix RNA binding column, filtered, washed, and eluted. Contaminating DNA bound to the fiber matrix was removed by DNase digestion.

Previously published primers were used to amplify α4 and α6 subunit mRNAs.[17] Additional primers were designed to amplify mRNAs of the α3, α5, α7, α9, β2, β3, and β4 nAChR subunits using primer design software (Primer Premier V. 5.0; Premier Biosoft, Palo Alto, CA). The sequences were designed against the cytoplasmic loop of human cDNA sequences obtained from GenBank (National Center for Biotechnology Information, Bethesda, MD; http//:www.ncbi.nlm.nih.gov). Primer sequences are listed in Table 1. Primers were synthesized by Invitrogen (Carlsbad, CA) or Sigma Genosys (The Woodlands, TX).

An RT-PCR kit (OneStep RT-PCR; Qiagen, Inc., Valencia, CA) was used for RT-PCR of retinal RNA. Briefly, primers and template RNA were mixed into RT-PCR buffer containing dNTPs and RT-PCR enzyme mix containing reverse transcriptases and *Taq* DNA polymerase. Template RNA was omitted as a negative control. Reverse transcription occurred at 50°C for 30 minutes, followed by 1 cycle at 95°C for 15 minutes to inactive the reverse transcriptases and activate the *Taq* polymerase. Denaturing, annealing, and extension consisted of 35 to 40 cycles at 94°C for 1 minute, 55°C to 60°C for 1.5 minutes and 72°C for 2 minutes, respectively. Final extension took place at 72°C for 20 minutes. Gel electrophoresis was used to separate RT-PCR products on 2% agarose gels with ethidium bromide visualization of the bands.

For further characterization, appropriately sized products were gel purified using a purification kit (QIAquick PCR Purification Kit; Qiagen Inc., Valencia, CA). Briefly, agarose segments containing DNA were dissolved in a proprietary buffer (QG; Qiagen), mixed with isopropanol, and centrifuged. DNA was captured on a DNA binding matrix and eluted with DEPC-treated H_2O. The purified DNA was sequenced (Center for AIDS Research, University of Alabama at Birmingham, Birmingham, AL) using both forward and reverse primers. The forward and reverse sequences were aligned with one another using a multiple sequence alignment program (Clustal W; European Bioinformatics Institute, Cambridge, UK; http://www.ebi.ac.uk/clustalw/) and compared to known DNA sequences through GenBank in an NCBI 'BLAST' query. The homologies of the amplified sequences from monkey retina to the appropriate human DNA sequences ranged from 93% to 99% without significant homology to other DNA sequences (Table 1).

Tissue Preparation for Immunohistochemistry

Fifteen enucleated eyes from ten rhesus monkeys were opened at the pars plana, immersion-fixed in ice-cold 2% paraformaldehyde or periodate-lysine-paraformaldehyde in 0.1M phosphate buffer for 2 to 4 hours, and then transferred into ice-cold 30% sucrose in 0.1M phosphate buffer for at least 48 hours. Each eye was hemisected in the region of the ora serrata, and the vitreous body was removed from the posterior segment. The posterior segments were embedded in a specimen matrix (Tissue-Tek O.C.T.; Sakura Finetek USA, Inc., Torrance, CA), frozen in liquid nitrogen, and transversely sectioned at 12 to 16 μm.

Antibodies

Thirteen well-characterized and specific monoclonal antibodies (mAbs) against the α3, α4, α6, α7, β2, or β4 subunit of the nACh receptor were used (see Table 2).

Immunohistochemistry

Tissue sections were routinely blocked for 30 minutes with the normal serum of the same species in which the secondary antibody was generated or with TNB solution (0.1M Tris-HCl, 0.15M NaCl, 0.5% blocking reagent) provided with the tyramide signal amplification kit (TSA kit, PerkinElmer, Waltham, MA; http://las.perkinelmer.com/ApplicationsSummary/Applications/Tyramide-Signal-Amplification.htm), a technique to enhance the visualization of immunolabeling. Tissue sections treated with the TSA kit were incubated with 0.3% hydrogen peroxide in methanol for 30 minutes to inactivate endogenous hydrogen peroxidase before applying the blocking reagent. The tissue sections were then incubated with the primary antibody overnight at room temperature, rinsed with TNT (0.1M Tris-HCl, 0.15 M NaCl, 0.3% Triton) buffer and then incubated for 1 hour in biotinylated goat

Table 1. RT-PCR of nAChR Subunits in Monkey Retina

nAChR Subunit	Primer Sequence	Annealing Temperature (°C)	Product Size (bp)	Product Homology to the Human Subunit Sequence
α3	Sense CAAGCAACGAGGGCAACG Antisense CCGTCCTGGCAGGGGTAG	60	121	97%
α4	Sense GTTCCATGACGGGCGGGTGCAGTGGACT Antisense GGGATGACCAGTGAGGTGGACGGGATGAT	58	482	98%
α5	Sense TTTCTTCACACGCTTCCCAAA Antisense TCACGGACATCATTTTCCTTCA	60	179	97%
α6	Sense ACCAATTTGTGGCTGCGTCAC Antisense CCAGAGATGTGGATGGGATGGT	58	652	97%
α7	Sense GGGAACCTGCTGTACATCGGC Antisense GGTGCTCATCGTGCGTGGG	60	115	93%
α9	Sense ATTCCCTGTGATCTATTCCAATGTT Antisense CAGTCACCCACCACTACGGTG	55	213	94%
β2	Sense CATCATTGCGCCCGTCAGC Antisense TCTGGTCATCGTCCTCGCTCC	60	277	95%
β3	Sense TTGGAAAAAGCTGCTGATTCC Antisense GGTAAAAATCAGAACCGAGCC	55	168	99%
β4	Sense AGCAAGTCATGCGTGACCAAG Antisense GCTGACACCTTCTAATGCCTCC	60	210	94%

TABLE 2. Antibodies Used for Immunohistochemistry

Subunit	Monoclonal Antibody[1,32,33]	Species Immunized	Working Concentration (μg/mL)
$\alpha3$	35	Rat	1×10^{-2}
	210	Rat	5×10^{-3}
$\alpha4$	299	Rat	1.2×10^{-2}
	369	Mouse	1.25×10^{-3}
	371	Mouse	1.25×10^{-3}
$\alpha6$	350	Mouse	1.1×10^{-2}
	351	Mouse	1×10^{-2}
$\alpha7$	306	Mouse	8×10^{-3}
	307	Rat	5.8×10^{-3}
	319	Rat	5.0×10^{-3}
$\beta2$	290	Rat	1×10^{-2}
	295	Rat	7×10^{-3}
$\beta4$	337	Mouse	5×10^{-3}

anti-rat or anti-mouse immunoglobulin (secondary antibody, Jackson Immunoresearch, West Grove, PA), depending on the original species of the primary antibody. The TSA reagents then were applied, following the manufacturer's instructions (peroxidase-conjugated strepavidin 1:200 for 30 minutes, and then biotin-conjugated tyramide 1:100 for 3 minutes). The immunoreactivity was visualized by incubation with strepavidin-conjugated Cy3 (Jackson ImmunoResearch) diluted 1:1800 for 25 minutes. To control for the specificity of secondary antibody, tissue sections were prepared by omitting the primary antibody. To control for the specificity of the primary antibody, tissue sections were prepared by substituting matched protein concentrations of normal serum of the species in which the primary antibody was generated. Tissue sections were covered in mounting in medium (Fluoromount-G; Southern Biotechnology Associates, Inc., Birmingham, AL) and observed by a fluorescence microscope (Nikon Microphot-SA; Nikon, Tokyo, Japan). Digital images were captured with a digital camera and imaging software (DXM1200 and ACT-1 version 2.20, respectively; both from Nikon).

RESULTS

RT-PCR Analysis

To determine the compliment of nAChR subtypes detectable in neural Rhesus monkey retina at the transcription level, RT-PCR that relied on primers designed from human nAChR nucleotide sequences was used. Products of the predicted size for $\alpha3$-$\alpha7$, $\alpha9$, and $\beta2$-$\beta4$ (Fig. 1) were detected and were subsequently sequenced to confirm identity. Homology between transcripts amplified from Rhesus monkey retina and human nucleotide sequences ranged from 93% to 99% (Table 1). There was variability in comparing the intensity of the product bands for each subunit, with the $\alpha4$ subunit band being the most intense and the $\alpha9$ product being the least intense. While these differences in the intensity of the product bands may reflect differences in the abundance of native mRNA transcripts for a given subunit, unequal transcription efficiencies may also have contributed to dissimilar band intensities.

Immunohistochemistry

Although the RT-PCR results suggested that the majority of nAChR subunits are expressed in Rhesus monkey retina, antibodies suitable for immunohistochemistry were available only for the $\alpha3$ to 4, $\alpha6$ to 7, and $\beta2$ and $\beta4$ nAChR subunits (Table 2). As RT-PCR had identified mRNA transcripts for each of these latter nAChR subunits, immunohistochemistry also identified these same subunits in specific cells of the monkey retina. While the intensity of labeling differed between eyes, the cellular patterns of immunoreactivity for each specific subunit were highly consistent between eyes. Based on their appearance on tissue sections, labeled cells are described as small (7 to 10 μm in diameter), medium (11 to 14 μm in diameter) or large (15 μm or greater in diameter); but these descriptive terms are not intended to imply size-dependent differences in labeled cell populations.

***α3* Subunit.** A moderate number of apparent amacrine cells in the inner nuclear layer (INL) and cells in the ganglion cell layer (GCL) displayed $\alpha3$ immunoreactivity, as did two well-defined bands of processes within the inner plexiform layer (IPL). These two distinct bands of labeled processes were found in *sublamina a* and *sublamina b* of the IPL. Many cone photoreceptors in the outer retina also were visualized (Fig. 2). While the outer segments were labeled most intensely, the entire cone photoreceptor showed immunoreactivity for the $\alpha3$ nAChR subunit. Small, round labeled somata in the INL were found predominantly in the innermost tier of cells, with occasional labeled somata visible in the second tier of the cells. Processes from some of these labeled neurons in the INL were visible as they entered the IPL and merged into the outer band of labeled processes. Fewer cells in the GCL were immunolabeled, and their distribution was uneven. Most cells were round or ovoid in shape and varied in size from small to large; they were seen either as isolated cells or as two or three cells close together. A short, thin process from the labeled somata was also occasionally visualized, extending to the inner band of labeled processes in the IPL. In the NFL, a few isolated nerve fibers were weakly labeled.

***α4* Subunit.** Many round or ovoid shaped, medium or large sized cells in the GCL displayed immunoreactivity to the $\alpha4$ nAChR subunit (Fig. 3). No processes from these cells could be visualized clearly. Only a very few medium-sized cells in the INL were labeled, and these were scattered in the innermost layer of the INL. No immunoreactivity was visualized in the IPL, but fibers in the NFL were weakly labeled.

***α6* Subunit.** The $\alpha6$ nAChR subunit was detected in cells with the typical morphology of microglial cells. They were distributed in the OPL, IPL, GCL, or NFL and were frequently, but not always, visualized in proximity to retinal blood vessels (Fig. 4). In vertical tissue sections the round, small cells in the OPL gave rise to processes that originated from each pole and extended along the OPL. In tangential sections, these cells appeared to be multipolar with three to five radially oriented processes confined to a narrow plane parallel to the retina surface. The processes from the cells in the OPL did not appear

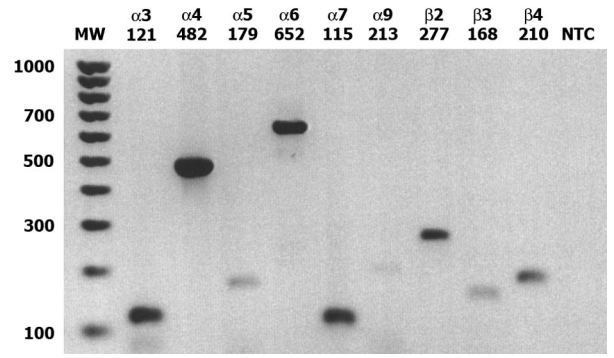

FIGURE 1. RT-PCR of nAChR subunit transcripts in monkey retina. mRNA transcripts for nAChR subunits $\alpha3$-$\alpha7$, $\alpha9$, and $\beta2$-$\beta4$ were amplified from neural Rhesus monkey retina. *Lane 1*: 100 base molecular weight marker. *Lanes 2- 9*: nAChR subunit product bands. *Lane 11*: No template control. Products of the predicted size were sequenced to confirm identity. Homology with human nAChR sequences ranged from 93% to 99% (Table 1).

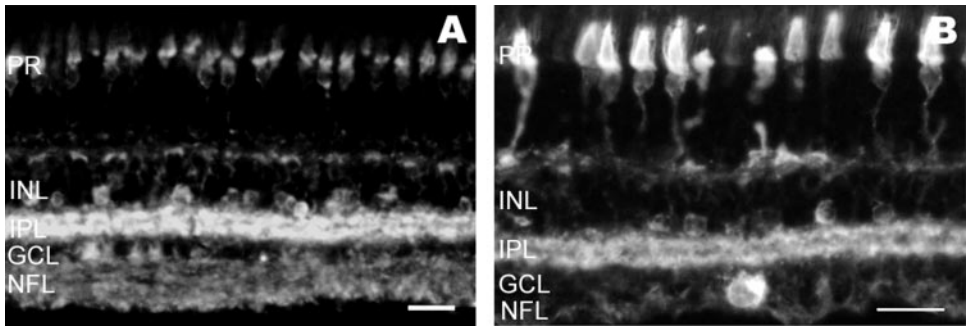

FIGURE 2. α3 nAChR subunit immunolabeling in monkey retina. (**A**, **B**) The overall distribution of α3-immunoreactive neurons is shown. Many cones, a moderate number of somata in the INL, and fewer somata in the GCL were labeled. Two intensely labeled bands in the IPL were observed. In some preparations, the NFL was weakly labeled (**A**); but in most cases, only a few isolated nerve fibers were immunoreactive. PR, photoreceptors. Scale bars, 25 μm.

to overlap. The majority of α6 nAChR immunoreactive cells were localized in the IPL. Labeling was visualized in all layers of the IPL, in contrast to the narrow distribution in the OPL. The IPL cells demonstrated variable morphology, with round, ovoid, or irregular somata of small to medium sizes and multiple branching processes. Also in contrast to the cells in the OPL, the labeled processes of the presumed microglia in the IPL could be observed to touch, overlap or even be entangled with those of nearby cells. Similar features were observed in the α6 nAChR immunoreactive microglia of the GCL and NFL, but these cells were in lower density and with less ramified, more symmetric processes.

***α*7 Subunit.** α7 nAChR subunit immunoreactivity was observed in cells in both the INL and GCL (Fig. 5). The majority of labeled cells in the INL were located either in the inner region near the IPL or, less frequently, in the outer region near the OPL. A few processes from these cells were visualized and traced to the adjacent plexiform layer. The cells in the inner INL were presumably amacrine cells, though the identities of the labeled cells in the outer tiers were less certain. Most cells in the GCL were medium to large sized neurons of round or ovoid shape, but a few small to medium sized neurons were also labeled. No nerve fibers from the immunoreactive GCL cells were labeled. A small number of medium to large sized immunoreactive cells were also displaced in the IPL.

***β*2 Subunit.** Many somata in the GCL and fewer somata in the INL displayed β2 nAChR subunit immunoreactivity (Fig. 6). Two broad, dense bands of labeled processed were visible in *sublamina a* and *b* of the IPL. The cells in the GCL were round or ovoid shaped and generally were larger than those in the INL. Some very short processes originating from the immunoreactive somata were labeled and projected into the IPL, while others could be seen entering the NFL; however, these fibers could be followed for only short distances. The larger cells in the GCL were presumably ganglion cells. The NFL was diffusely and intensely labeled, but the intense immunoreactivity terminated abruptly in the region of the posterior margin of the lamina cribrosa.

***β*4 Subunit.** Many cells were immunoreactive for the β4 nAChR subunit and displayed the morphologic characteristics of microglia. The β4 nAChR -immunoreactive cells were distributed in the OPL, IPL, GCL, and NFL (Fig. 7) in a pattern very similar to that of the labeling for the α6 subunit (Fig. 5). Processes of immunoreactive cells in the OPL ramified in a plane parallel to the retinal surface. In addition, β4 nAChR subunit immunoreactive cells were extensively distributed throughout the IPL, with processes arborizing within the IPL or the adjacent INL. Antibodies to the nAChR subunit also labeled a small number of cells in the GCL and NFL with similar morphologic features.

DISCUSSION

These results demonstrate that transcripts for most nAChR subunits, presumably representing nAChRs of varying subunit composition, are expressed by neurons in the retina of Rhesus monkey. RT-PCR analysis yielded products of the predicted size for α3–α7, α9, and β2-β4 subunits. The products were sequenced and homology between transcripts amplified from Rhesus monkey retina and human nucleotide sequences ranged from 93% to 99% (Table 1). By immunohistochemistry using specific monoclonal antibodies, various retinal cell types were immunoreactive for the α3, α4, α6, α7, β2, and β4 nAChR subunits, indicating protein product expression for these particular subunits. As in reported in other species,[16,19–22,34,35] the retina of Rhesus monkey thus expresses a diversity of nAChR subunits, in complex cellular expression patterns.

Immunoreactivity for β2, α3, α4, and α7 subunits was detectable in cells in the inner INL with the morphologic appearance of amacrine cells. Although which putative amacrine cell types express nAChRs in the Rhesus monkey retina has yet to be determined, subpopulations of amacrine cells in rabbit retina, including GABAergic and glycinergic amacrine cells, also express α3, β2, and α7 nAChR subunits.[19,21,22] Glycinergic cells in the mammalian retina are typically small field cells that synapse more frequently with amacrine and ganglion cells than with bipolar cells.[36–39] Therefore, the activation of nAChRs on glycinergic amacrine cells in the monkey retina may be a mechanism for modulating the release of

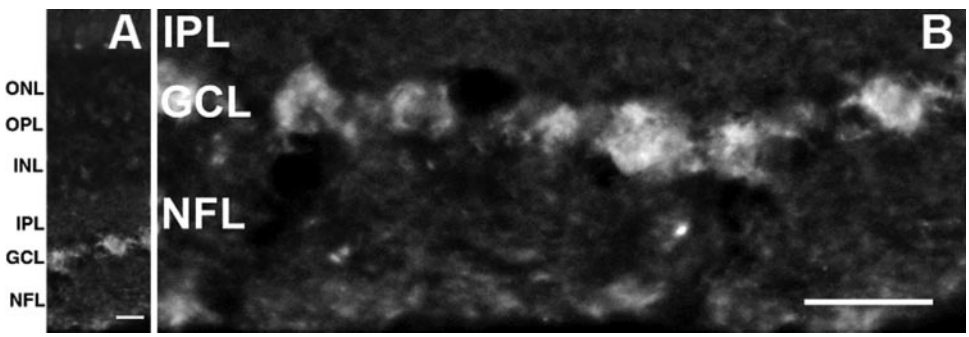

FIGURE 3. α4 nAChR subunit immunolabeling in monkey retina. (**A**) A micrograph of the entire retinal thickness demonstrates that the GCL was the predominant location for cells immunoreactive to α4 nAChR subunit antibodies. (**B**) Many immunoreactive cell somata are seen in the GCL, likely corresponding to ganglion cells. The immunostained cells in (**A**) correspond to the two cells on the *right* side of (**B**). NFL labeling was irregular and tended to be weak. Scale bars: (**A**) 10 μm; (**B**) 25 μm.

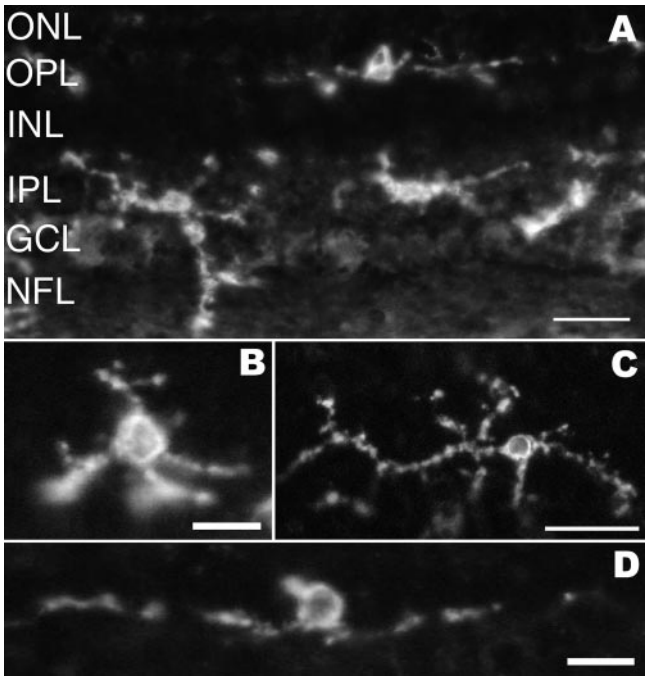

FIGURE 4. α6 nAChR subunit immunolabeling in monkey retina. (**A**) As illustrated here in a vertical tissue section, the α6 nAChR subunit localized to cells with irregularly shaped somata and processes distributed in both plexiform layers, the GCL and NFL. These cells have the appearance of retinal microglial cells. (**B**) A putative microglial cell in the IPL is shown. The somata in the IPL demonstrated variable shapes and sizes, with complex ramifications of their processes. (**C**) In an obliquely oriented tissue section, an immunoreactive cell in the OPL appeared multipolar with radially oriented processes. (**D**) A labeled microglial cell in the OPL in a vertical tissue section is shown, illustrating that the cells in the OPL are confined within a narrow plane parallel to the retinal surface. Scale bars: (**A**, **E**) 25 μm; (**B**, **C**, **D**) 10 μm.

inhibitory neurotransmitters onto other subpopulations of amacrine cells.

The present study does not unambiguously establish the identity of outer INL cells labeled by antibodies against the α7 subunit. That these might be immunoreactive bipolar cells is an intriguing observation because of a previous report in non-human primate retina showing that cholinergic cells synapse directly onto cone bipolar cell terminals, in addition to synapsing on amacrine and ganglion cells.[40] More recently, α7 nAChRs were also detected in ON cone bipolar cells of rabbit retina.[22] Some of these labeled cells displayed calbindin immunoreactivity, others were labeled for calbindin and glycine, while still others exhibited only glycine immunoreactivity, indicating that α7 nAChRs are expressed by at least three distinct subpopulations of ON-cone bipolar cells. These findings add to reports over nearly three decades that nAChRs are expressed by bipolar cells. Specifically, observations in chick,[41] mouse,[42] goldfish,[43] and turtle[44] all demonstrated αBgt binding associated with bipolar cells or amacrine-bipolar synapses. Another study showed αBgt-sensitive nAChR (α8 subunits) antibody labeling of bipolar cells in the avian retina.[45]

The retina includes circuits for rod-mediated scotopic and cone-mediated photopic vision. Rods and cones synapse onto one type of rod bipolar cell and many types of cone bipolar cells, respectively, and specific types of cone bipolar cells make synaptic contacts with specific subtypes of ganglion cells. However, the rod signal carried by rod bipolar cells can reach ganglion cells only by passing first to AII amacrine cells that in turn synapse onto cone bipolar cells.[39,46] In rabbit retina, there is evidence that nAChRs are involved primarily in the photopic pathway.[22] Taken together, these results justify future efforts to establish the identity of the α7-positive outer INL cells and the participation of nAChRs in specific circuits in the non-human primate retina.

Cells in the GCL expressing nAChRs also were detected in the monkey retina, specifically the β2, α3, α4, and α7 subunits. Based on the size and shape of the labeled cells, many are likely to be ganglion cells. By immunoprecipitation, in situ hybridization and/or radioligand binding, the α6 nAChR subunit has been detected at significant levels in retinal ganglion cells, their axons and/or their central axon terminals in rat or chick[16,34,35,47]; but we observed no α6 immunolabeling of presumed ganglion cells in monkey retinal tissue sections. RT-PCR of whole retina, while identifying the α6 nAChR transcript, cannot establish cellular origin; and we would now not assert clear species differences in the expression by retinal ganglion cells of the α6 nAChR subunit given potential technical issues with immunohistochemistry on monkey tissues. Previous studies of the rabbit retina have revealed both α7- and β2-containing neurons in the GCL. In rabbit, some ganglion cells express α7 and α3β2 nAChRs and others exhibit α7 immunoreactivity only.[22] Many physiologically identified GC types, including subsets of sustained OFF and sustained ON, transient OFF[17] and some directionally selective ON-OFF cells, may express β2-containing and α7 nAChRs.[14,18] The responses of other subsets of ganglion cells to the applications of cholinergic agonists were mediated solely by α7 nAChRs.[17] These data, together with the physiological studies cited above, suggest that ACh can directly affect the responses of ganglion cells through the activation of α7 nAChRs and/or β2-containing nAChRs on the GCs themselves, as well as on the upstream cells.

The significance of the apparent expression of nAChRs by cone photoreceptors in non-human primate retinas is unclear. There are reports that choline acetyltransferase is expressed in the cones of amphibian and turtle retina[48]; but to our knowledge, no data suggest functional nicotinic cholinergic circuitry in the outer retina of mammals.

Antibodies against the α6 and β4 nAChR subunits labeled cells that resembled microglia. Functional nAChR subtypes containing α6 and β4 subunits have been described in hippocampus.[49] Additionally, there are numerous reports of neuronal nAChR subtype expression and function in non-neuronal cells, including endothelial cells, epithelial cells, and keratino-

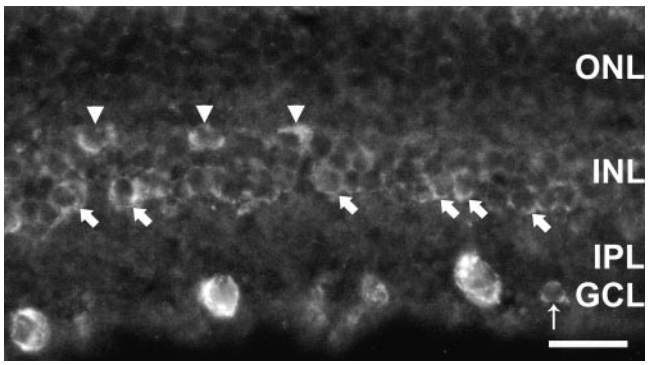

FIGURE 5. α7 nAChR subunit immunolabeling in monkey retina. The α7 nAChR subunit localized to some cells in both the INL and GCL. Many cells in the inner tier (*thick arrows*) and some cells in the outer tier (*arrowheads*) of the INL were labeled. Cells in the GCL were generally large compared to those in the INL, but a few small cells were occasionally visualized in the GCL (*narrow arrow*). Scale bar, 25 μm.

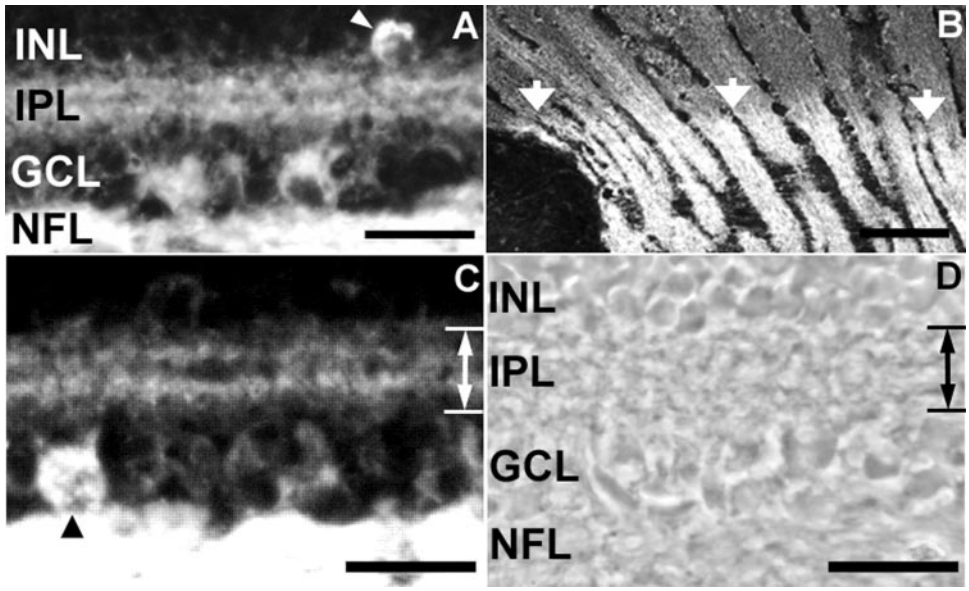

FIGURE 6. β2 nAChR subunit immunolabeling in monkey retina. (**A**) The distribution of β2-immunoreactive neurons is shown. Many somata in the GCL and fewer somata in the INL (*arrow head*) were immunoreactive. Two immunoreactive bands were visible in the IPL, and the NFL was diffusely labeled. (**B**) The intense immunoreactivity of the nerve fiber layer terminated abruptly in the region of the posterior margin of the lamina cribrosa (*arrows*). (**C**, **D**) Corresponding fluorescence (**C**) and phase (**D**) micrographs at higher magnification illustrate the relationship of the immunolabeled bands and the IPL. The breadth of the IPL is shown by the *double arrow* at the right edge of each field. In (**C**), note also the strongly immunoreactive ganglion cell (*arrowhead*), some more weakly labeled ganglion cells and the intensely labeled NFL. Scale bars: (**A**,**C**, **D**) 25 μm; (**B**) 100 μm.

cytes.[50–52] Recent evidence indicates that microglia have a mesodermal origin, and thus a lineage distinct from that of macroglia that are derived from neuroectoderm.[53]

In initial studies on human retina with a similar immunohistochemical approach (data not shown), antibodies to α4 and α7 nAChR subunits labeled various neuronal somata; but immunohistochemical reactivity to the other subunits was not detected. While demonstrating that human retina expresses at least two nAChR subunits, postmortem changes and the long fixation times of the available donated human tissue preclude direct comparison to the monkey data. Evaluating fresh or weakly fixed human retinas for nAChR subunits would comprise a worthwhile future study.

Evolving recent evidence also links nAChR function to pathologic processes in the eye. Refractive development seems governed by a visual feedback mechanism located in large part in the retina,[54] and nicotinic cholinergic mechanisms comprise one of the pharmacologic pathways implicated in the development of refractive errors in experimental animals[29] and possibly in children.[30,31] Nicotinic cholinergic mechanisms, perhaps acting at vascular endothelial cells, influence experimental retinal neovascularization and may provide a novel therapeutic pathway for age-related macular degeneration.[28] While most prior interest in ACh signaling in non-retinal eye physiology and ocular pathology has addressed muscarinic ACh receptors,[55] new observations are both highlighting the potential importance of nAChRs and suggesting new opportunities in cholinergic pharmacology.

In summary, the apparent expression of diverse nAChRs by different classes of retinal neurons in the non-human primate retina suggests effects at several stages of visual information processing. The release of ACh from cholinergic amacrine cells may boost the responses of ON- and ON-OFF types of ganglion cells through the activation of postsynaptic nAChRs on ganglion cells themselves. The activation of nAChRs expressed by inhibitory amacrine cells that synapse with other inhibitory amacrine cells likely would cause inhibition or disinhibition of multiple circuits and may exert a variety of effects on specific types of ganglion cells. The activation of nAChRs on bipolar cells could modulate bipolar cell output onto ganglion cells. Finally, recent observations suggest that nicotinic cholinergic signaling in the retina may influence not only visual processing

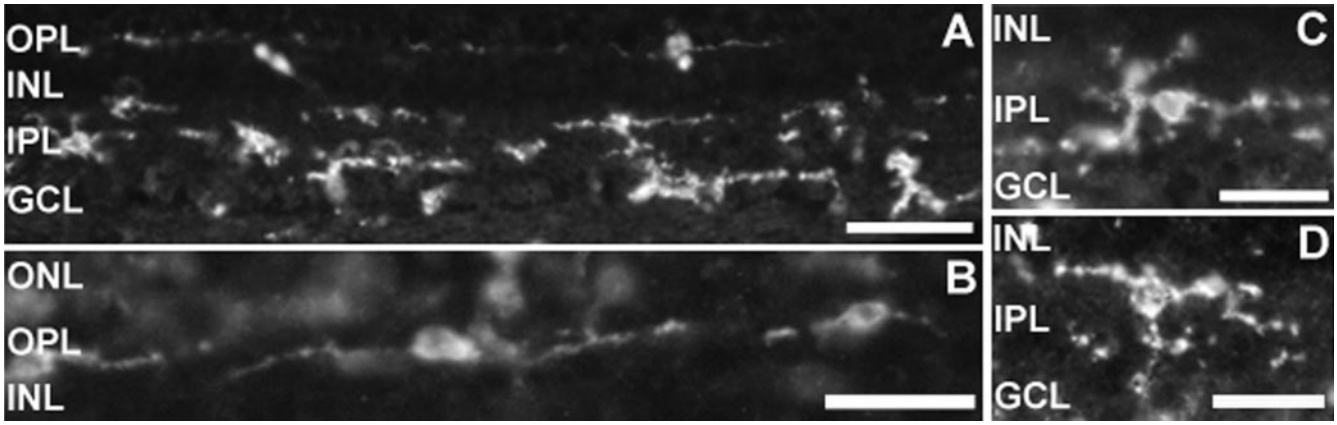

FIGURE 7. β4 nAChR subunit immunolabeling in monkey retina. (**A**) The β4 nAChR subunit distribution. Many cells in the OPL, IPL, GCL and NFL were labeled in a pattern very similar to that observed for the α6 subunit (see Fig. 5). (**B**) Labeled cells in the OPL with their processes. These cells appeared confined to a narrow plane within the OPL parallel to the surface of the retina. (**C**, **D**) Two labeled cells in the middle part of the IPL and their processes. The shapes and sizes of the cell somata and processes varied considerably. Scale bars: (**A**) 50 μm; (**B**, **C**, **D**) 25 μm.

but also normal ocular development and certain ocular pathologies.

References

1. Lindstrom J. The structures of neuronal nicotinic receptors. In: Clementi F, Fornasari D, Gotti C., eds. *Neuronal Nicotinic Receptors. Handbook of Experimental Pharmacology*. Vol. 144. Berlin: Springer; 2000:101–162.
2. Dani JA. Overview of nicotinic receptors and their roles in the central nervous system. *Biol Psychiatry.* 2001;49:166–174.
3. Millar NS, Harkness PC. Assembly and trafficking of nicotinic acetylcholine receptors (review). *Mol Membr Biol.* 2008;25:279–292.
4. Gotti C, Clementi F. Neuronal nicotinic receptors: from structure to pathology. *Prog Neurobiol.* 2004;74:363–396.
5. Masland RH, Mills JW, Cassidy C. The functions of acetylcholine in the rabbit retina. *Proc R Soc Lond B Biol Sci.* 1984;223:121–139.
6. Vaney DI. 'Coronate' amacrine cells in the rabbit retina have the 'starburst' dendritic morphology. *Proc R Soc Lond B Biol Sci.* 1984;220:501–508.
7. Masland RH, Livingstone CJ. Effect of stimulation with light on synthesis and release of acetylcholine by an isolated mammalian retina. *J Neurophysiol.* 1976;39:1210–1219.
8. Masland RH, Ames A, 3rd. Responses to acetylcholine of ganglion cells in an isolated mammalian retina. *J Neurophysiol*. 1976;39:1220–1235.
9. Ariel M, Daw NW. Effects of cholinergic drugs on receptive field properties of rabbit retinal ganglion cells. *J Physiol.* 1982;324:135–160.
10. Ariel M, Daw NW. Pharmacological analysis of directionally sensitive rabbit retinal ganglion cells. *J Physiol.* 1982;324:161–185.
11. Ikeda H, Sheardown MJ. Acetylcholine may be an excitatory transmitter mediating visual excitation of 'transient' cells with the periphery effect in the cat retina: iontophoretic studies in vivo. *Neuroscience.* 1982;7:1299–1308.
12. Schmidt M, Humphrey MF, Wässle H. Action and localization of acetylcholine in the cat retina. *J Neurophysiol.* 1987;58:997–1015.
13. Jurklies B, Kaelin-Lang A, Niemeyer G. Cholinergic effects on cat retina in vitro: changes in rod- and cone-driven b-wave and optic nerve response. *Vis Res.* 1996;36:797–816.
14. Reed BT, Amthor FR, Keyser KT. Rabbit retinal ganglioin cell responses mediated by α-bungarotoxin-sensitive nicotinic acetylcholine receptors. *Vis Neurosci.* 2002;19:427–438.
15. Strang CE, Amthor FR, Keyser KT. Rabbit retinal ganglion cell responses to nicotine can be mediated by beta2-containing nicotinic acetylcholine receptors. *Vis Neurosci.* 2003;20:651–662.
16. Moretti M, Vailati S, Zoli M, et al. Nicotinic acetylcholine receptor subtypes expression during rat retina development and their regulation by visual experience. *Mol Pharmacol.* 2004;66:85–96.
17. Strang CE, Andison ME, Amthor FR, Keyser KT. Rabbit retinal ganglion cells express functional α7 nicotinic acetylcholine receptors. *Am J Physiol Cell Physiol.* 2005;289:C644–655.
18. Strang CE, Renna JM, Amothor FR, Keyser KT. Nicotinic acetylcholine receptor expression by directionally selective ganglion cells. *Vis Neurosci.* 2007;24:523–533.
19. Keyser KT, MacNeil MA, Dmitrieva NA, Wang F, Masland RH, Lindstrom JM. Amacrine, ganglion, and displaced amacrine cells in the rabbit retina express nicotinic acetylcholine receptors. *Vis Neurosci.* 2000;17:743–752.
20. Dmitrieva NA, Lindstrom JM, Keyser KT. The relationship between GABA-containing cells and the cholinergic circuitry in the rabbit retina. *Vis Neurosci.* 2001;18:93–100.
21. Dmitrieva NA, Pow DV, Lindstrom JM, Keyser KT. Identification of cholinoceptive glycinergic neurons in the mammalian retina. *J Comp Neurol.* 2003;456:167–175.
22. Dmitrieva NA, Strang CE, Keyser KT. Expression of alpha 7 nicotinic acetylcholine receptors by bipolar, amacrine, and ganglion cells of the rabbit retina. *J Histochem Cytochem.* 2007;55:461–476.
23. Zak PP, Lelekova TV. [The effect of acetylcholine on the membrane potential of goldfish retina horizontal cells and the frog electroretinogram]. *Neirofiziologiia.* 1975;7:55–59.
24. Jardon B, Yucel H, Bonaventure N. Glutamatergic separation of ON and OFF retinal channels: possible modulation by glycine and acetylcholine. *Eur J Pharmacol.* 1989;162:215–224.
25. Jardon B, Bonaventure N, Scherrer E. Possible involvement of cholinergic and glycinergic amacrine cells in the inhibition exerted by the ON retinal channel on the OFF retinal channel. *Eur J Pharmacol.* 1992;210:201–207.
26. Von Bredow J, Bay E, Adams N. Drug actions on the central nervous system as studied by the effects on the electroretinogram. *Exp Neurol.* 1971;33:45–52.
27. Antal A, Keri S, Bodis-Wollner I. L-alpha-glycerylphosphorylcholine enhances the amplitude of the pattern electroretinogram in rhesus monkeys. A pilot study. *Neurobiology (Bp).* 1999;7:407–412.
28. Kiuchi K, Matsuoka J, Wu JC, et al. Mecamylamine suppresses basal and nicotine-stimulated choroidal neovascularization. *Invest Ophthalmol Vis Sci.* 2008;49:1705–1711.
29. Stone RA, Sugimoto R, Gill AS, Liu J, Capehart C, Lindstrom JM. Effects of nicotinic antagonists on ocular growth and experimental myopia. *Invest Ophthalmol Vis Sci.* 2001;42:557–565.
30. Saw S-M, Chia K-S, Lindstrom JM, Tan DTH, Stone RA. Childhood myopia and parental smoking. *Brit J Ophthalmol.* 2004;88:934–937.
31. Stone RA, Wilson LB, Ying G-S, et al. Associations between childhood refraction and parental smoking. *Invest Ophthalmol Vis Sci.* 2006;47:4277–4287.
32. Kuryatov A, Luo J, Cooper J, Lindstrom J. Nicotine acts as a pharmacological chaperone to up-regulate human alpha4beta2 acetylcholine receptors. *Mol Pharmacol.* 2005;68:1839–1851.
33. Tumkosit P, Kuryatov A, Luo J, Lindstrom J. Beta3 subunits promote expression and nicotine-induced up-regulation of human nicotinic alpha6 nicotinic acetylcholine receptors expressed in transfected cell lines. *Mol Pharmacol.* 2006;70:1358–1368.
34. Vailati S, Moretti M, Longhi R, Rovati GE, Clementi F, Gotti C. Developmental expression of heteromeric nicotinic receptor subtypes in chick retina. *Mol Pharmacol.* 2003;63:1329–1337.
35. Cox BC, Marritt AM, Perry DC, Kellar KJ. Transport of multiple nicotinic acetylcholine receptors in the rat optic nerve: high densities of receptors containing α6 and β3 subunits. *J Neurochem.* 2008;105:1924–1938.
36. Pourcho RG, Goebel DJ. A combined Golgi and autoradiographic study of ^{3}H-glycine-accumulating amacrine cells in the cat retina. *J Comp Neurol.* 1985;233:473–480.
37. MacNeil MA, Masland RH. Extreme diversity among amacrine cells: implications for function. *Neuron.* 1998;20:971–982.
38. Menger N, Pow DV, Wässle H. Glycinergic amacrine cells of the rat retina. *J Comp Neurol.* 1998;401:34–46.
39. Kolb H. How the retina works. *Am Sci.* 2003;91:28–35.
40. Yamada ES, Dmitrieva N, Keyser KT, Lindstrom JM, Hersh LB, Marshak DW. Synaptic connections of starburst amacrine cells and localization of acetylcholine receptors in primate retinas. *J Comp Neurol.* 2003;461:76–90.
41. Vogel Z, Maloney GJ, Ling A, Daniels MP. Identification of synaptic acetylcholine receptor sites in retina with peroxidase-labeled alpha-bungarotoxin. *Proc Natl Acad Sci USA.* 1977;74:3268–3272.
42. Pourcho RG. Localization of cholinergic synapses in mammalian retina with peroxidase-conjugated alpha-bungarotoxin. *Vision Res.* 1979;19:287–292.
43. Zucker C, Yazulla S. Localization of synaptic and nonsynaptic nicotinic-acetylcholine receptors in the goldfish retina. *J Comp Neurol.* 1982;204:188–195.
44. James WM, Klein WL. alpha-Bungarotoxin receptors on neurons isolated from turtle retina: molecular heterogeneity of bipolar cells. *J Neurosci.* 1985;5:352–361.
45. Keyser KT, Britto LR, Schoepfer R, et al. Three subtypes of α-bungarotoxin-sensitive nicotinic acetylcholine receptors are expressed in chick retina. *J Neurosci.* 1993;13:442–454.
46. Bloomfield SA, Dacheux RF. Rod vision: pathways and processing in the mammalian retina. *Prog Retin Eye Res.* 2001;20:351–384.

47. Perry DC, Mao D, Gold AB, McIntosh JM, Pezzullo JC, Kellar KJ. Chronic nicotine differentially regulates α6- and β3-containing nicotinic cholinergic receptors in rat brain. *J Pharmacol Exp Ther.* 2007;322:306–315.
48. Blute TA, Strang C, Keyser KT, Eldred WD. Activation of the cGMP/nitric oxide signal transduction system by nicotine in the retina. *Vis Neurosci.* 2003;20:165–176.
49. Azam L, McIntosh JM. Characterization of nicotinic acetylcholine receptors that modulate nicotine-evoked [3H]norepinephrine release from mouse hippocampal synaptosomes. *Mol Pharmacol.* 2006;70:967–976.
50. Grando SA, Horton RM, Pereira EF, et al. A nicotinic acetylcholine receptor regulating cell adhesion and motility is expressed in human keratinocytes. *J Invest Dermatol.* 1995;105:774–781.
51. Grando SA. Biological functions of keratinocyte cholinergic receptors. Journal of Investigative Dermatology, Symposium Proceedings. *J Invest Dermatol Symp Proc.* 1997;2:41–48.
52. Wang Y, Pereira EF, Maus AD, et al. Human Bronchial Epithelial and Endothelial Cells Express alpha 7 Nicotinic Acetylcholine Receptors. *Mol Pharmacol.* 2001;60:1201–1209.
53. Chan WY, Kohsaka S, Rezaie P. The origin and cell lineage of microglia: new concepts. *Brian Res Rev.* 2007;53:344–354.
54. Stone RA. Myopia pharmacology: etiologic clues, therapeutic potential. In: Yorio T, Clark A, Wax M, eds. *Ocular Therapeutics: An Eye on New Discoveries*. New York: Elsevier/Academic Press; 2007:167–196.
55. Nietgen GW, Schmidt J, Hesse L, Hönemann CW, Durieux ME. Muscarinic receptor functioning and distribution in the eye: molecular basis and implications for clinical diagnosis and therapy. *Eye.* 1999;13:285–300.